


RESEARCH ARTICLES

Open Access



Colonic oxygen microbubbles augment systemic oxygenation and CO₂ removal in a porcine smoke inhalation model of severe hypoxia

Paul A. Mountford^{1†}, Premila D. Leiphakpam^{2†}, Hannah R. Weber², Andrea McCain², Robert M. Scribner¹, Robert T. Scribner¹, Ernesto M. Duarte³, Jie Chen², Dragana Noe², Mark A. Borden^{1,4} and Keely L. Buesing^{1,2,5*} 

[†]Paul A. Mountford and Premila D. Leiphakpam contributed equally to this work.

*Correspondence: keely.buesing@unmc.edu

¹ Respirogen, Inc., Boulder, CO, USA

² University of Nebraska Medical Center, Omaha, NE, USA

³ University of Florida College of Medicine, Gainesville, FL, USA

⁴ University of Colorado Boulder, Boulder, CO, USA

⁵ Department of Surgery, 983280 Nebraska Medical Center, University of Nebraska Medical Center, Omaha, NE 68198-3280, USA

Abstract

Inhalation injury can lead to pulmonary complications resulting in the development of respiratory distress and severe hypoxia. Respiratory distress is one of the major causes of death in critically ill patients with a reported mortality rate of up to 45%. The present study focuses on the effect of oxygen microbubble (OMB) infusion via the colon in a porcine model of smoke inhalation-induced lung injury. Juvenile female Duroc pigs ($n = 6$ colonic OMB, $n = 6$ no treatment) ranging from 39 to 51 kg in weight were exposed to smoke under general anesthesia for 2 h. Animals developed severe hypoxia 48 h after smoke inhalation as reflected by reduction in SpO₂ to $66.3 \pm 13.1\%$ and PaO₂ to 45.3 ± 7.6 mmHg, as well as bilateral diffuse infiltrates demonstrated on chest X-ray. Colonic OMB infusion (75–100 mL/kg dose) resulted in significant improvements in systemic oxygenation as demonstrated by an increase in PaO₂ of 13.2 ± 4.7 mmHg and SpO₂ of $15.2 \pm 10.0\%$ out to 2.5 h, compared to no-treatment control animals that experienced a decline in PaO₂ of 8.2 ± 7.9 mmHg and SpO₂ of $12.9 \pm 18.7\%$ over the same timeframe. Likewise, colonic OMB decreased PaCO₂ and PmvCO₂ by 19.7 ± 7.6 mmHg and 7.6 ± 6.7 mmHg, respectively, compared to controls that experienced increases in PaCO₂ and PmvCO₂ of 17.9 ± 11.7 mmHg and 18.3 ± 11.2 mmHg. We conclude that colonic delivery of OMB therapy has potential to treat patients experiencing severe hypoxemic respiratory failure.

Introduction

Prior to the spread of SARS-CoV-2, acute respiratory distress syndrome (ARDS) historically occurred in ~10% of patients entering the intensive care unit—affecting nearly 190,000 patients per year in the US alone—with a reported mortality rate ranging from 35 to 46% [1, 2]. As of March 2023, a total of 1.3 million COVID-19 deaths have been reported in the US [3]. The primary symptom of COVID-19 infection requiring hospitalization is hypoxemic respiratory failure [4]. Regardless of underlying pathology, mechanical ventilation remains the mainstay of oxygenation and ventilatory support for severe respiratory failure; however, complications such as ventilator-induced lung injury,

ventilator-associated pneumonia, barotrauma, and progressive deconditioning leading to ventilator dependence remain unacceptably high [5]. Despite decades of research, therapeutic options for patients with severe hypoxemia that fail mechanical ventilatory support are limited.

Oxygen microbubble (OMB) therapy is a novel technology that shows promise as a method of extrapulmonary oxygenation that is relatively simple and safe to administer, does not require the use of anticoagulants and has a low risk profile. OMB comprises a high concentration of micron-scale (1–20 μm diameter) bubbles that contain an oxygen “core” and are encapsulated by a lipid monolayer shell [6], similar to the pulmonary alveolus. When administered into the abdominal cavity (akin to peritoneal dialysis), OMBs have been reported to augment systemic oxygenation and improve outcome in small animal pilot studies involving unilateral pneumothorax, tracheal occlusion, and LPS-mediated severe ARDS [6–8].

Here, we introduce a novel delivery pathway for OMB therapy—the colon—as an improved translational candidate for minimally invasive, nonsurgical systemic oxygenation and carbon dioxide removal. The colonic mucosa is associated with a rich capillary matrix. Oxygen tension in the mucosal layer has been studied in small animal models of hyperbaric oxygen therapy, where investigators found that oxygen diffused from intestinal tissue and established a radial gradient from the tissue interface to the colonic lumen [9]. It naturally follows that if systemic hyperoxia can augment luminal oxygen content via the capillary gradient, establishing an elevated oxygen content in the colonic lumen would lead to diffusion across the capillary bed, augmenting systemic oxygenation in states of hypoxemia. A similar argument holds for carbon dioxide removal due to the same capillary gradient. Moreover, the colon provides an ability to deliver a clinically relevant volume of OMB without the need to place a surgical port, as required by alternative routes studied to date. This study examines the hypothesis that colonic OMB therapy can significantly increase systemic oxygen levels and reduce systemic carbon dioxide levels in a large-animal model of severe hypoxia.

Materials and methods

Note from authors: The first draft of this manuscript has been published on the preprint server, bioRxiv.com [10].

Animal subjects

All animal experiments were approved by the University of Nebraska Lincoln (UNL) Institutional Animal Care and Use Committee (IACUC). Female pigs (31–51 kg, randomized to $n=6$ treatment, $n=6$ no treatment) were housed and cared for according to USDA (United States Department of Agriculture) guidelines. A sample size of 6 per group was chosen based upon our previous work with OMB therapy, which showed significance in treatment effect versus no treatment at this sample size [6–8]. Animals were acclimated to the facility for 4–7 days and received food reward training to ease handling and blood draws. Study animals were fasted overnight and given free access to water for procedures on the following day.

Animal preparation and surgical procedures

Sedation for peripheral intravenous catheter (PIV) placement and endotracheal intubation was achieved with a mixture of telazol (4.4 mg/kg), ketamine (2.2 mg/kg) and xylazine (2.2 mg/kg) delivered via intramuscular injection. To assist with intubation, an intravenous bolus dose of propofol (2–4.4 mg/kg) was given as needed. Baseline chest X-ray (CXR) (Fig. 1A, B) was obtained (portable X-ray unit EPX-F2800, Ecotron Co. Ltd; wireless digital flat panel detector Mars1417V-TSI, iRay Technology, Shanghai, China) prior to smoke inhalation, and at 24 and 48 h after smoke inhalation (Fig. 1D, E). Animals were not ventilated again until the morning of the treatment day, allowing the injury to develop over 48 h. On the morning of treatment day, an endotracheal tube (#7–8 cuffed; MWI Animal Health, Boise, ID, USA) was inserted into the trachea and animals were ventilated at a tidal volume (TV) of approximately 6 mL/kg (6.07 ± 0.38 mL/kg, $n = 12$) and positive end expiratory pressure (PEEP) of 5 cm H₂O (Newport HT70, Medtronic, Minneapolis, MN). Respiratory rate (RR) was adjusted to maintain eucapnia as monitored by end-tidal CO₂ (ETCO₂), and defined as less than 50 mmHg. The fraction of inspired oxygen (FiO₂) was set at 0.50 during surgical procedures (central venous catheter placement and arterial catheter placement), then titrated down to 0.21 (equivalent

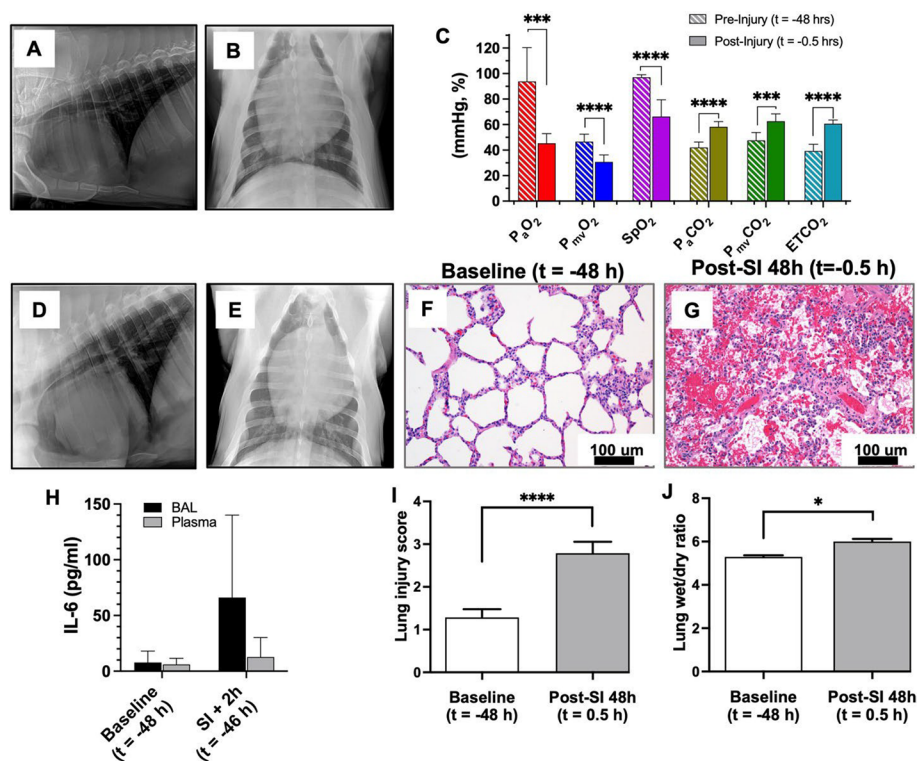


Fig. 1 Porcine smoke inhalation injury. **A, B** Before and after (**D, E**) chest X-ray images confirming the presence of diffuse bilateral infiltrates indicative of ARDS due to smoke inhalation injury. **C** P_aO₂ (red, $p = 0.000147$), P_{mv}O₂ (blue, $p < 0.0001$), SpO₂ (violet, $p < 0.0001$), P_aCO₂ (gold, $p < 0.0001$), P_{mv}CO₂ (green, $p = 0.000123$) and ETCO₂ (teal, $p < 0.0001$) measurements taken both before ($t = -48$ h) and after ($t = -0.5$ h) smoke inhalation injury. Hematoxylin and eosin (H&E) staining of paraffin-embedded lung tissue sections of baseline ($t = -48$ h) (**F**) and SI + 48 h ($t = -0.5$ h) (**G**) animals (scale bar = 100 μ m). **H** IL-6 marker analysis for baseline and smoke injury (SI) + 2 h ($t = -46$ h) for BAL and plasma samples. Comparison of lung injury score (**I**) and lung wet/dry ratios (**J**) showing a significant difference between control and SI + 48 h ($t = -0.5$ h) samples ($p < 0.0001$ and $p = 0.0188$, respectively)

of room air) and maintained throughout the experiment. Non-invasive monitoring included blood pressure taken by cuff placed around the animal's hind leg, peripheral oxygen saturation (SpO_2), heart rate (HR) and $ETCO_2$ recorded via the Surgivet monitor (Smiths Medical, Dublin, OH). Continuous IV sedation consisting of midazolam (0.4–0.7 mg/kg/h), fentanyl (0.03–0.1 mg/kg/h) and/or propofol (0.2–0.4 mg/kg/min), and maintenance IV fluids (10 mL/kg/h normal saline) were given throughout the procedure via a quadruple-lumen central venous catheter (8.5 Fr \times 16 cm, Arrow International) placed in the external jugular vein under ultrasound guidance. Core temperature was monitored by rectal probe and a circulating warming blanket was used to prevent body cooling. A urinary catheter was placed to monitor output. Using sterile technique and ultrasound guidance (Butterfly iQ, Butterfly Network, New York City, NY), carotid artery (CA) and femoral artery (FA) access catheters were placed for serial lab draws and invasive blood pressure monitoring (18 GA 16 cm; Femoral Arterial Line Catheterization Kit; Teleflex, Morrisville, NC). Pulmonary artery (PA) catheter (8 Fr \times 110 cm Swan-Ganz CCombo Thermodilution Catheter; Edwards Lifesciences, Irvine, CA) was placed in the external jugular vein (on the side opposite the quadruple-lumen catheter) under ultrasound guidance and advanced to the pulmonary artery as confirmed by waveform. The CA and PA access ports were connected to Surgivet monitor and Vigilance II monitor (Edwards Lifesciences, Irvine, CA), respectively, with transducers (Meritans DTX-Plus, Disposable Pressure Transducer with EasyVent; Merit Medical, South Jordan, UT, USA). Invasive arterial blood pressure (ABP), central venous pressure (CVP), pulmonary artery pressure (PAP), cardiac output (CO), mixed venous oxygen saturation ($S_{mv}O_2$), and central (core) temperature were monitored throughout the study. Blood samples were drawn from the CA, FA and PA catheters for the measurement of baseline blood gas prior to smoke inhalation and at pre-determined time intervals throughout the study period (ABL80 FLEX CO-OX, Radiometer, Brea, CA). To maintain patency, catheters were flushed throughout the experiment with 3–5 mL of sterile saline, and a heparin solution (1:500 dilution in 50% dextrose solution) was infused to fill the volume of the port chosen as a "lock" solution. Sedated/anesthetized animals from survival surgeries were continuously monitored until they regained sternal recumbency. All catheters were removed after smoke inhalation was completed, to prevent dislodgement by the animals during the subsequent 48 h. The surgical procedures were repeated at 48 h after smoke inhalation using the same technique, prior to treatment with OMBs.

Smoke inhalation

Upon completion of all surgical procedures, animals ($n = 12$) were exposed to oak wood smoke from a custom-made smoke generator connected in parallel to the endotracheal tube. The duration of the smoke exposure was 2 h, and the volume of smoke was approximately 1000 L (as estimated from TV, RR, and total time of smoke exposure). Invasive and non-invasive vital signs were monitored continuously during the experiment. Following smoke exposure, blood samples were collected from CA, FA and PA ports for blood gas analysis. Smoke exposure was stopped immediately if the animal developed hemodynamic instability, which was determined by hypotension (systolic blood pressure less than 60 mmHg) and irreversible desaturation (SpO_2 less than 70% despite

rescue maneuvers such as increasing FiO_2). Details of our smoke exposure protocol are included in previous publication [11].

Oxygen microbubble preparation

OMBs were generated via sonication as described by Feshitan et al. [6]. The resulting OMB solution, which contained 15% oxygen gas by total volume [void fraction (VF)=0.15], was then centrifuged (Sorvall Legend T, Thermo Scientific, Waltham, MA) as described by Swanson et al. [9] in batches of four 140 mL syringes (Covidien Monoject 140, Medtronic, Minneapolis, MN) at 300 relative centrifugal force (RCF) for 1 min to achieve a final oxygen gas content of $VF \geq 0.7$ (+70% oxygen gas by total volume). The resulting high-concentration oxygen microbubble foam was collected in 2-L gas-tight syringes (S2000, Hamilton, Reno, NV) and stored at $\sim 4^\circ\text{C}$. OMB size (Fig. 2A) was

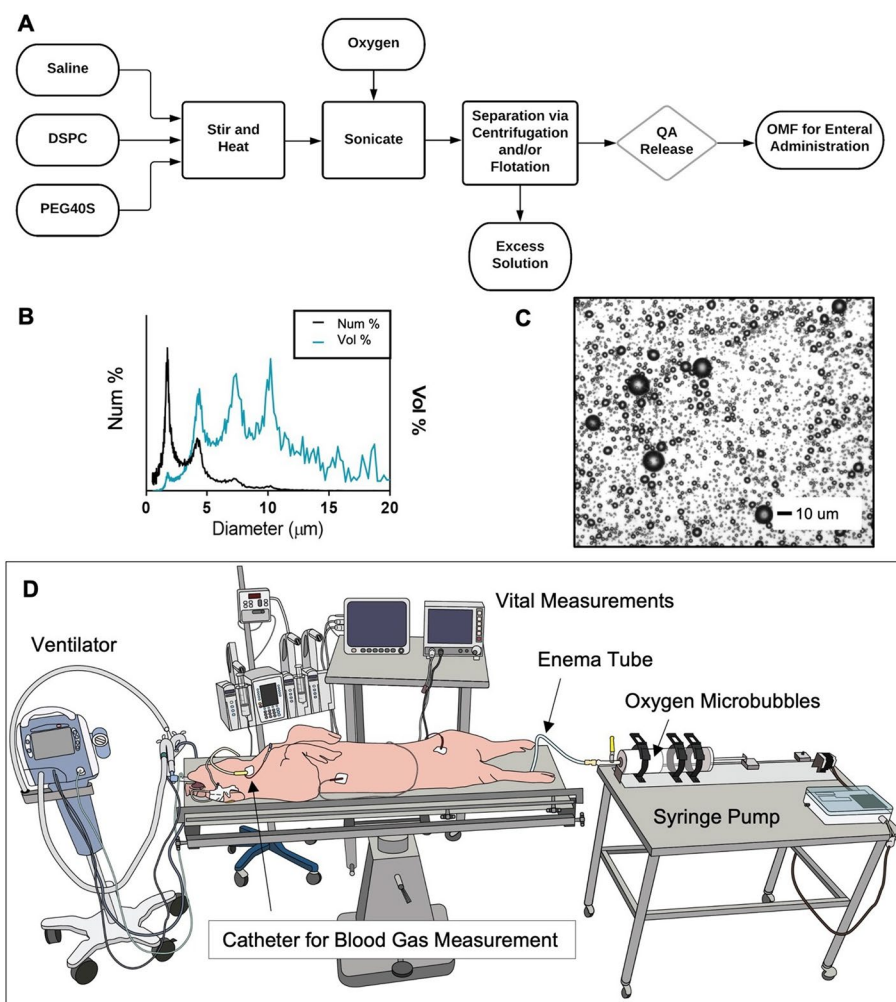


Fig. 2 Colonic OMB administration. **A** Process flow diagram showing the production process for creating OMB via sonication and differential centrifugation (DSPC = distearoylphosphatidylcholine, PEG40S = polyoxyethylene 40 stearate, QA = quality assurance, OMF = oxygen microfoam). **B** Particle size by both number percent (black) and volume percent (blue) frequency for the OMB samples. **C** Microscopy image showing the size of the OMB (scale bar = 10 μm). **D** Schematic showing the colonic delivery of OMB to a smoke inhalation lung injured pig on minimal mechanical ventilation ($FiO_2 = 0.21$)

measured using the electrozone sensing method (Coulter Multisizer III, Beckman Coulter, Opa Locka, FL). OMB VF was calculated by subtracting the weight of a fixed volume of OMB from the weight of an equivalent volume of aqueous solution (lipid–PBS mixture) and dividing by the weight of the aqueous solution at the same fixed volume. Finally, oxygen gas content by total gas volume (%) was measured with an oxygen needle sensor (OX-NP, Unisense, Aarhus, Denmark).

No treatment and colonic oxygen microbubble treatment

At 48 h after smoke inhalation, CXR was obtained and CA, FA, and PA catheters were again placed for serial blood sampling and monitoring as described above. Lung injury from smoke inhalation was confirmed by presence of bilateral diffuse infiltrates on CXR (Fig. 1D, E). After completion of catheter placement, FiO_2 was lowered to 0.21 and maintained throughout the remainder of the experiment. Other ventilator parameters were set to $TV=6-8$ mL/kg, $PEEP=0-1$ to maintain normal driving pressure (defined as less than 15 mmHg, as suggested in current literature for patients with ARDS/ALI [12–15]), and RR was adjusted to maintain eucapnia. Baseline blood gas samples (CA, PA and FA ports) were taken every 15 min until the desired level of hypoxia was achieved ($P_aO_2 \leq 45 \pm 5$ mmHg). After three consecutive hypoxic blood gas measurements ($P_aO_2 \leq 45 \pm 5$ mmHg) at 5-min intervals, animals receiving OMB treatment ($n=6$) had a rectal tube (super xl enema kit, Bracco Diagnostics Inc. Monroe Township, NJ) placed, the occlusive balloon inflated, and a purse string suture secured around the anus to ensure a tight seal of the enema tube (Fig. 2D). The enema tubing was then connected to the 2-L super syringe containing the OMB. The OMB were delivered to the animal at a rate of 500 mL/min which was controlled by a custom syringe pump (Respirogen, Boulder, CO). A total dose of 75–100 mL/kg of OMB therapy was delivered to the study animals (for example, at 100 mL/kg a 45 kg animal would receive a 4.5-L dose), equivalent to the dose used in our prior work focusing on peritoneal delivery of OMB therapy [8]. We paused delivery two times during therapy administration to assess abdominal distension, tolerance of therapy as measured by respiratory and hemodynamic parameters, and change syringes. Animals receiving no treatment ($n=6$) had a theoretical treatment time ($t=0$ min) ~ 5 min after their last baseline measurement.

Following treatment ($t=0$ min), arterial and mixed-venous blood gas samples were taken at $t=15, 30, 45, 60, 90, 120,$ and 150 min post-treatment time. After the experiments, animals were euthanized with an intravenous injection of 0.1 mL/lb of Fatal-Plus (Vortech Pharmaceuticals, Dearborn, MI).

Plasma sample extraction

Blood samples were collected from the CA catheter at baseline, 2 h, and 48 h time points in lithium heparin BD Microtainer tubes (Becton, Dickinson and Company, Franklin Lakes, NJ). Tubes were immediately inverted 8–10 times to assure anticoagulation and centrifuged at $4000 \times g$ for 3 min. Supernatants were collected as plasma samples and stored at -20 °C until analysis. IL-6, IL1 β and IL-8 immune assays were performed in samples of 12 animals using IL-6 (catalog#P6000B), IL1 β /IL-1F2 (catalog#PLB00B) and IL-8/CXCL8 (catalog#P8000) Quantikine[®] ELISA kits, (R&D Systems, Inc., Minneapolis, MN) following manufacturer's protocol.

Bronchoalveolar lavage (BAL)

BAL of pig lungs was performed at baseline, 2 h, and 48 h time points using a bronchoscope in our 12 intubated animals. A total of 10 mL of sterile normal saline was instilled to the secondary and tertiary bronchi through the bronchoscope and ~5 mL of the fluid was collected for analysis. BAL fluid samples were centrifuged immediately at $400\times g$ at 4 °C for 10 min and supernatants were stored at -20 °C until analysis. Total protein quantification was performed in samples using Pierce™ BCA (bicinchoninic acid) Protein Assay Kit (Thermo Fisher Scientific Inc. Waltham, MA) following manufacturer's protocol. IL-6, IL1 β and IL-8 immune assays were performed in samples of 12 animals using IL-6 (catalog#P6000B), IL1 β /IL-1F2 (catalog#PLB00B) and IL-8/CXCL8 (catalog#P8000) Quantikine® ELISA kits, (R&D Systems, Inc., Minneapolis, MN) following manufacturer's protocol.

Tissue collection

Necropsy was performed in all study animals. Lung tissue was collected from all five lobes: upper, middle and lower lobes of right lung and upper and lower lobes of left lung for histological examination and pulmonary edema assessment. Tissues for histology were immediately placed in 10% neutral buffer formalin fixative for approximately 24 h. Formalin-fixed tissues were placed into 70% ethanol and transferred to the University of Nebraska Medical Center (UNMC) Tissue Science Facility (TSF) for further tissue processing and embedment in paraffin blocks.

Lung injury score

Lung tissue from all study animals, preserved after necropsy in 10% neutral formalin, was dehydrated in graded concentrations of ethanol solution and cleared in xylene. The tissue samples were then paraffin-embedded, sectioned with 4- μ m thickness, and stained with hematoxylin and eosin at the UNMC Tissue Sciences Facility using automated Ventana Discovery Ultra (Roche Diagnostics, Indianapolis, IN) as per manufacturer's protocol. An independent pathologist performed a blinded examination of the tissues under light microscopy. Ten fields of each lung tissue section were examined at magnification 40 \times . The severity of the lung injury was scored by the criteria of alveolar edema, intra-alveolar hemorrhage, and leukocyte infiltration. Alveolar edema and intra-alveolar hemorrhage were scored on a scale from 0 to 3; where 0 \leq 5% of maximum pathology, 1 = mild (< 10%), 2 = moderate (10–20%), and 3 = severe (20–30%). Leukocyte infiltration was also scored on a scale from 0 to 3; where 0 = absence of extravascular leukocytes, 1 \leq 10, 2 = 10–45, and 3 \geq 45 leukocytes.

Lung tissue lysate preparation

Lung tissue with highest injury score ($n=9$) were homogenized using VWR® Mini Bead Mill Homogenizer (VWR International LLC., Radnor, PA) following manufacturer's protocol. Briefly, frozen tissues of three control, three SI animals and three SI + OMB animals were washed in cold X1 PBS, and 30 mg of each tissue was placed separately in a 2 mL tube containing 2.8 mm ceramic beads and 750 μ L of lysis buffer containing RIPA buffer (Thermo Fisher Scientific Inc. Waltham, MA) and protease

inhibitor cocktail (Sigma Aldrich Inc., St. Louis, MO) at room temperature. The samples were homogenized at speed 4 for 60 s. This was followed by incubation in ice for 30 min and centrifugation at 13,000 rpm for 20 min at 4 °C. Protein concentration was determined using Pierce™ BCA (Bicinchoninic Acid) Protein Assay Kit (Thermo Fisher Scientific Inc. Waltham, MA) following manufacturer's protocol.

Immunoblot analysis

Protein (50 µg) was separated by SDS-polyacrylamide gel electrophoresis and transferred onto polyvinylidene fluoride (PVDF) membrane (Bio-Rad Lab Inc., Hercules, CA) by electro blotting. The PVDF membrane was blocked with 5% nonfat dry milk in X1 TBST (50 mM Tris, pH 7.5, 150 mM NaCl, 0.01% Tween 20) for 1 h at room temperature (RT). The membrane was then incubated in primary antibody, IL-6 antibody (#ab6672, Abcam Inc, Cambridge, MA) and IL-1β (#P420B, Thermo Fisher Scientific, Waltham, MA) or β-actin (#4970, Cell Signaling Technology Inc., Danvers, MA) at 1:1000 dilution in X1 TBST with 5% bovine serum albumin (Sigma Aldrich Inc., St. Louis, MO) overnight at 4 °C. The membrane was washed three times with X1 TBST for 10 min each and incubated with HRP-conjugated rabbit or mouse secondary antibodies (#7074 and #7076, Cell Signaling Technology Inc., Danvers, MA) at 1:5000 dilution in X1 TBST with 5% nonfat dry milk for 1 h at RT. Following three washes in X1 TBST, proteins were detected using the enhanced chemiluminescence system (Bio-Rad Lab Inc, Hercules, CA) and image with ChemiDoc™ MP Imaging System (Bio-Rad Lab Inc, Hercules, CA).

Sample preparation for mass spectrometry

The protein concentration in the cell lysates was estimated using BCA Protein Assay Kit (Pierce) for each sample. The protein digestion for mass spectrometry and TMT labeling of the peptides were carried out following the manufacturer's suggestions. Briefly, 100 µg of proteins from each lysate was reconstituted to 100 µL with 100 mM triethylammonium bicarbonate (TEAB). Proteins were next reduced with 5 µL of 200 mM tris(2-carboxyethyl) phosphine (TCEP) (1 h incubation, 55 °C) and alkylated with 5 µL of 375 mM iodoacetamide (IAA) (30 min incubation in the dark, room temperature). The reduced and alkylated proteins were purified with acetone precipitation at –20 °C overnight. The protein precipitates were collected by centrifugation at 8000×g for 10 min at 4 °C. The pellets were air-dried and resuspended in 100 µL of 50 mM TEAB. Next, the protein digestion was carried out using 2.5 µg of trypsin per sample (24 h incubation, 37 °C). The amount of peptide yielded in each sample was estimated with the Pierce Colorimetric Peptide Assay kit. The amounts of peptides to be tagged were normalized and mixed with 41 µL of TMT reagent (TMT sixplex, Thermo Fisher Sci) freshly dissolved in acetonitrile (20 µg/µL) (1 h incubation, room temperature). 8 µL of 5% hydroxylamine was added to quench the reaction (15 min incubation, room temperature). Tagged tryptic peptides were pooled and concentrated to around 20 µL by vacuum centrifugation and analyzed using a high-resolution mass spectrometry nano-LC–MS/MS Tribrid system, Orbitrap Fusion™ Lumos™ coupled with UltiMate 3000 HPLC system (Thermo Scientific).

LC-MS/MS and bioinformatics analysis

Approximately 1 µg of peptides were run on the pre-column (Acclaim PepMap™ 100, 75 µm × 2 cm, nanoViper, Thermo Scientific) and the analytical column (Acclaim PepMap™ RSCL, 75 µm × 50 cm, nanoViper, Thermo Scientific). The peptides were eluted using a 125-min linear gradient of ACN (0–45%) in 0.1% FA and introduced to the mass spectrometer with a nanospray source. The MS scan was done using detector: Orbitrap resolution 120,000; scan range 375–1500 *m/z*; RF lens 60%; AGC target 5.0×10^5 ; maximum injection time 150 ms. Ions with intensity higher than 5.0×10^3 and charge state 2–7 were selected in the MS scan for further fragmentation. MS2 scan parameters set: CID collision energy 35%; activation Q 0.25; AGC target 1.0×10^4 ; maximum injection time 150 ms. MS3 scan parameters were set: HCD collision energy 65%; Orbitrap resolution 50,000; scan range 100–500 *m/z*; AGC target 1.0×10^5 , maximum injection time 200 ms. All MS and MSn collected spectra were analyzed using Protein Discoverer (Thermo Fisher Sci, vs 2.2.) pipeline. Sequest HT was set up to search the NCBI database (selected for *Sus scrofa*, 2019_01, 63,657 entries), assuming the digestion enzyme trypsin. The parameters for Sequest HT were set as follows: Enzyme: trypsin, Max missed cleavage: 2, Precursor mass tolerance: 10 ppm, Peptide tolerance: ± 0.02 Da, Fixed modifications: carbamidomethyl (C), TMT sixplex (any N-terminus); Dynamic modifications: oxidation (M), TMT sixplex (K). The parameters for Reporter ions quantifier were set as follows: integration tolerance: 20 ppm, integration method: most confident centroid, mass analyzer: FTMS, MS order: MS3, activation type: HCD, min. collision energy: 0. max. collision energy: 1000. Percolator was used to calculate the false discovery rate (FDR) for the peptide spectral matches. The parameters for Percolator were set as follows: target FDR (strict): 0.01, target FDR (relaxed): 0.05, validation based on: *q*-value. Quantification parameters were set: peptides to use: unique + razor, normalization mode: total peptide amount.

Alveolar oxygen pressure quantification

The alveolar pressure of oxygen in the lungs (P_AO_2) is the estimated amount of oxygen in the alveoli. The P_AO_2 for study animals was calculated with the equation

$$P_AO_2 = (P_b + MAP - P_{H_2O}) * FiO_2 - (P_aCO_2/RQ),$$

where P_b is the atmospheric pressure (760 mmHg), MAP is the mean airway pressure, P_{H_2O} is the water vapor pressure (47 mmHg) and RQ is the respiratory quotient (0.8), and is presented in Fig. 6 [16, 17].

Adverse events

Necropsy was performed after humane euthanasia for all animals. There were no adverse events such as colon perforation seen in any study animals. Abdominal distension was observed in the study animals as a result of colonic OMB injection; however, this did not result in significant change to respiratory parameters such as peak or plateau airway pressures, which would prompt concern for intraabdominal hypertension or abdominal

compartment syndrome. As there was no effect on pulmonary physiologic parameters as a result of colonic OMB injection, intraabdominal pressure was not measured.

Statistics analysis

Statistical analysis was completed using Prism 9 (GraphPad, San Diego, CA). All oxygen and CO₂ blood gas data are reported as mean ± standard deviation. Statistical significance for pre- and post-injury blood gas comparisons in Fig. 1C was based on an unpaired parametric *t*-test with Welch correction (non-equal standard deviations). The mean ± standard deviation of the delta of the no-treatment group (*n* = 6) and the delta of the OMB treatment group (*n* = 6) at the -30, -15, 15, 30, 45, 60, 90, 120 and 150 min time points is presented in Table 1. Statistical significance for the colonic OMB delta plots was determined using a mixed effects model with multiple comparisons and the intergroup results are presented in Table 2.

Table 1 NT and colonic OMB sample sizes and oxygen and CO₂ measurements

Time post-treatment (min)	P _a O ₂ (mmHg)	P _a O ₂ /FiO ₂	P _{mv} O ₂ (mmHg)	SpO ₂ (%)	P _a CO ₂ (mmHg)	P _{mv} CO ₂ (mmHg)	ETCO ₂ (mmHg)	P _a O ₂ (mmHg)
No treatment (N=6)								
-3000 (48 h)	85.5 ± 5.2	407.1 ± 24.8	48.8 ± 5.8	96.1 ± 2.2	40.9 ± 4.8	45.6 ± 7.4	39.8 ± 6.1	98.6 ± 6.0
-30	57.8 ± 7.3	275.2 ± 34.8	38.3 ± 8.0	77.6 ± 11.8	53.9 ± 3.3	56.4 ± 5.6	56.5 ± 4.8	82.4 ± 4.1
-15	50.2 ± 7.0	239.1 ± 33.3	31.0 ± 6.8	61.3 ± 13.0	56.5 ± 3.1	60.2 ± 2.8	60.5 ± 3.9	79.1 ± 3.9
15	47.8 ± 10.7	227.6 ± 51.0	28.5 ± 8.0	58.5 ± 13.6	61.9 ± 4.3	66.4 ± 4.8	64.7 ± 5.5	72.3 ± 5.3
30	45.8 ± 13.6	218.1 ± 64.8	28.3 ± 10.4	54.9 ± 16.1	64.8 ± 4.3	68.2 ± 6.5	65.6 ± 6.1	68.8 ± 7.9
45	49.2 ± 12.4	234.3 ± 59.1	30.2 ± 10.0	55.8 ± 15.7	65.0 ± 5.8	69.1 ± 5.8	66.5 ± 7.5	68.5 ± 7.3
60	49.2 ± 10.5	234.3 ± 50.0	30.2 ± 10.1	57.1 ± 15.6	65.6 ± 6.0	67.7 ± 5.8	66.8 ± 5.6	67.8 ± 7.5
90	47.2 ± 8.4	224.8 ± 40.0	28.3 ± 9.1	54.2 ± 13.2	65.7 ± 5.7	70.8 ± 6.4	68.1 ± 6.7	67.6 ± 7.1
120	43.5 ± 12.1	207.1 ± 57.6	25.8 ± 10.8	46.9 ± 15.5	68.1 ± 7.4	73.4 ± 7.3	70.9 ± 8.1	64.6 ± 9.2
150	42.0 ± 10.8	200.0 ± 51.4	23.7 ± 10.6	48.5 ± 13.8	74.4 ± 11.9	78.5 ± 12.1	75.5 ± 11.1	56.7 ± 14.9
OMB treatment (N=6 unless stated otherwise)								
-3000 (48 h)	78.8 ± 21.9	375.2 ± 104.3	44.3 ± 5.6	97.8 ± 1.5	45.1 ± 2.8	49.6 ± 5.1 N=5	33.5 ± 4.8	93.4 ± 3.6
-30	44.3 ± 7.2	211.0 ± 34.3	27.8 ± 8.5	75.3 ± 13.2	65.4 ± 10.0	69.6 ± 7.6 N=5	59.0 ± 4.9	67.9 ± 12.5
-15	43.2 ± 7.2	205.7 ± 34.3	29.5 ± 4.4	71.5 ± 14.0	70.6 ± 8.4	75.0 ± 11.9 N=5	58.0 ± 5.4	61.5 ± 10.5
15	52.5 ± 6.7	250.0 ± 31.9	32.7 ± 5.6	81.2 ± 11.7	61.2 ± 6.4	74.9 ± 14.5 N=5	52.7 ± 6.7	73.2 ± 8.0
30	54.7 ± 10.9	260.5 ± 51.9	35.0 ± 10.4	80.8 ± 8.8	61.9 ± 7.4 N=5	73.4 ± 11.0 N=5	55.2 ± 2.8	72.3 ± 9.3 N=5
45	54.7 ± 12.7	260.5 ± 60.5	36.3 ± 10.2	82.0 ± 7.8	61.5 ± 4.5 N=5	75.3 ± 12.3 N=5	52.8 ± 3.8	72.9 ± 5.6 N=5
60	53.7 ± 10.7	255.7 ± 51.0	35.0 ± 10.8	85.7 ± 9.2	59.5 ± 4.4 N=5	68.1 ± 7.7 N=5	52.0 ± 3.1	75.3 ± 5.4 N=5
90	56.6 ± 10.2 N=5	269.5 ± 48.6 N=5	33.8 ± 10.0 N=5	86.3 ± 6.1 N=5	59.2 ± 6.8 N=5	66.0 ± 5.6 N=4	48.4 ± 5.0 N=5	75.7 ± 8.4 N=5
120	57.2 ± 10.6 N=5	272.4 ± 50.5 N=5	36.6 ± 8.9 N=5	88.6 ± 5.1 N=5	55.6 ± 6.3 N=5	63.8 ± 5.2 N=4	49.7 ± 4.2 N=5	80.1 ± 7.9 N=5
150	56.4 ± 7.9 N=5	268.6 ± 37.6 N=5	34.8 ± 5.8 N=5	89.4 ± 4.8 N=5	53.5 ± 5.6 N=5	64.2 ± 4.9 N=4	47.0 ± 6.4 N=5	82.8 ± 7.0 N=5

Animal oxygen and CO₂ blood gas measurements and counts for time points *t* = -3000, -30, -15, 15, 30, 45, 60, 90, 120 and 150 min for NT and colonic OMB treatment groups

Table 2 Colonic OMB mixed effects analysis

P_aO_2						$P_{mv}O_2$						SpO_2							
Fixed effects (type III)						Fixed effects (type III)						Fixed effects (type III)							
	DFn	DFd	F	P value		DFn	DFd	F	P value		DFn	DFd	F	P value		DFn	DFd	F	P value
Time	3.21	30.5	0.5267	0.6791	Time	2.771	26.33	1.066	0.3764	Time	2.731	25.94	0.7014	0.5471	Time	2.078	19.75	0.8246	0.4571
Treatment	1	10	26.58	0.0004	Treatment	1	10	8.313	0.0163	Treatment	1	10	7.593	0.0182	Treatment	1	10	33.81	0.0002
Time x treatment	6	57	2.418	0.0376	Time x treatment	6	57	2.101	0.0672	Time x treatment	6	57	2.983	0.0133	Time x treatment	6	57	5.926	<0.0001
Random effects	SD	Variance			Random effects	SD	Variance			Random effects	SD	Variance			Random effects	SD	Variance		
Subject	5.027	25.27			Subject	5.231	27.36			Subject	12.3	151.3			Subject	3.959	15.67		
Residual	4.63	21.44			Residual	3.761	14.14			Residual	6.417	41.17			Residual	4.065	16.52		
P_aCO_2						$P_{mv}CO_2$						$ETCO_2$							
Fixed effects (type III)						Fixed effects (type III)						Fixed effects (type III)							
	DFn	DFd	F	P value		DFn	DFd	F	P value		DFn	DFd	F	P value		DFn	DFd	F	P value
Time	2.254	18.41	0.1742	0.8647	Time	2.372	20.16	1.935	0.165	Time	2.078	19.75	0.8246	0.4571	Time	2.078	19.75	0.8246	0.4571
Treatment	1	9	56.57	<0.0001	Treatment	1	9	25.99	0.0006	Treatment	1	10	33.81	0.0002	Treatment	1	10	33.81	0.0002
Time x treatment	6	49	7.718	<0.0001	Time x treatment	6	51	7.867	<0.0001	Time x treatment	6	57	5.926	<0.0001	Time x treatment	6	57	5.926	<0.0001
Random effects	SD	Variance			Random effects	SD	Variance			Random effects	SD	Variance			Random effects	SD	Variance		
Subject	4.926	24.26			Subject	4.428	19.6			Subject	3.959	15.67			Subject	3.959	15.67		
Residual	4.074	16.6			Residual	3.836	14.71			Residual	4.065	16.52			Residual	4.065	16.52		

The mixed effects analysis for the colonic OMB treatment and no-treatment groups delta in measurement from baseline as plotted in Fig. 6C–H. The model assumes an alpha of 0.05 with no sphericity

The colonic OMB treatment group fell to an $n=5$ after 60 min due to a loss in data collection for one of the animals. The same animal had a loss in collection of P_aCO_2 data within 15 min of OMB treatment. An additional animal dataset did not contain $P_{mv}CO_2$ data due to equipment error bringing the $P_{mv}CO_2$ sample size from $n=5$ to $n=4$ after 60 min.

One-way ANOVA for multiple comparisons was used to compare control ($n=4$) vs. SI ($n=5$) vs. SI+OMB ($n=5$) samples for lung injury and wet/dry ratios. IL-1 β immunoblot analysis was performed on $n=3$ baseline samples and $n=4$ NT and OMB samples. IL-6 marker injury analysis was performed on $n=11$ animals for both baseline and 2-h post-smoke inhalation time points for both BAL and plasma samples. The IL-6 treatment analysis was performed on $n=6$ BAL samples and $n=5$ plasma samples for both the NT and OMB treatment groups 48-h post-SI injury.

Results

Lung injury due to smoke inhalation injury

Prior to OMB treatment at 48 h after smoke inhalation, lung injury was assessed by chest X-ray (CXR) and carotid, femoral and pulmonary arterial catheter blood gas sampling. CXR confirmed the presence of diffuse bilateral infiltrates indicative of ARDS (Fig. 1A–E). While on a fraction of inspired oxygen (FiO_2) level of 0.21 (oxygen content equivalent to room air), P_aO_2 decreased from 93.8 ± 26.5 mmHg to 45.3 ± 7.6 mmHg and SpO_2 dropped from $97.0 \pm 2.1\%$ to $66.3 \pm 13.1\%$, while P_aCO_2 rose from 42.0 ± 4.3 mmHg to 58.2 ± 4.1 mmHg at 30 min prior to OMB treatment (Fig. 1C). There was an increase in IL-6 inflammation within the lungs (Fig. 1H, BAL). Additionally, we observed a significant increase in overall lung injury score (Fig. 1I) and average wet–dry (W/D) weight ratio of lung tissues 48 h after smoke exposure compared to the control animals (Fig. 1J).

Systemic O_2 delivery and CO_2 removal

Upon achieving severe hypoxia due to smoke inhalation injury, OMB was administered to the colon (Fig. 2D) as described previously. The OMB had a number-weighted average microbubble diameter of 1–10 μ m with most of the oxygen gas volume existing in bubbles 1–2 μ m in diameter (Fig. 2B). Within 120 min after the start of OMB treatment, all blood and non-invasive oxygen vitals showed statistically higher oxygen content for animals receiving OMB treatment compared to no-treatment control animals. Specifically, P_aO_2 rose significantly for OMB-treated animals within the first 15 min to 52.5 ± 6.9 mmHg (OMB $\Delta P_aO_2 = 9.3 \pm 6.4$ mmHg, no treatment (NT) $\Delta P_aO_2 = -2.3 \pm 6.7$ mmHg) and continued rising to 56.4 ± 7.9 mmHg (OMB $\Delta P_aO_2 = 13.2 \pm 4.7$ mmHg, NT $\Delta P_aO_2 = -8.2 \pm 7.9$ mmHg) after 150 min (Fig. 3A, C). Additionally, $P_{mv}O_2$ increased significantly for OMB treatment animals to 34.8 ± 5.8 mmHg (5.0 ± 5.9 mmHg over -7.3 ± 6.9 mmHg as seen by the NT animals) after 150 min (Fig. 3A, D). SpO_2 also rose significantly by $14.2 \pm 9.5\%$ after 60 min as compared to the drop seen in the no-treatment group (NT $\Delta SpO_2 = -4.2 \pm 14.91\%$) and was statistically higher at 150 min (OMB $\Delta SpO_2 = 15.2 \pm 10.0\%$, NT $\Delta SpO_2 = -12.9 \pm 18.7\%$, Fig. 3A, E).

Moreover, arterial measurements showed blood gas CO_2 declining from treatment until the end of the study for animals receiving OMB. Specifically, P_aCO_2 (Fig. 3B, F) was significantly lower for animals receiving OMB after 15 min at 61.20 ± 6.39 mmHg

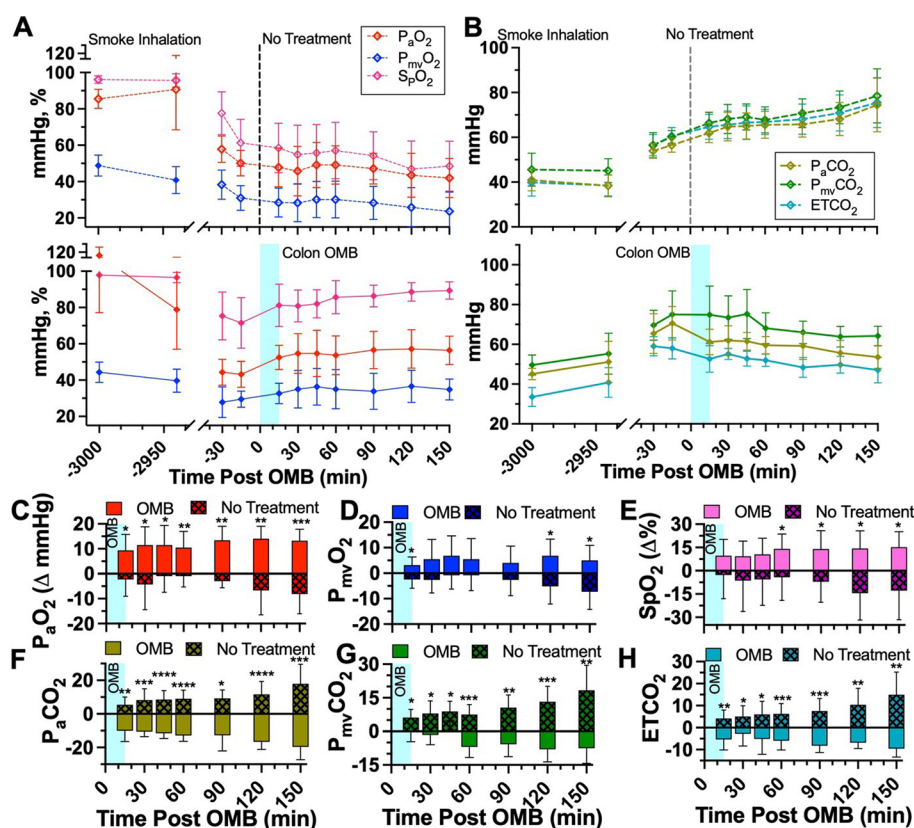


Fig. 3 Colonic OMB systemic oxygenation and CO₂ removal. **A** Blood oxygen and **B** CO₂ measurements for NT (top) and colonic OMB (bottom) treatment groups from before smoke inhalation injury ($t = -3000$ min) out to $t = 150$ min post-treatment time. The change in oxygen vitals for NT (hashed) and OMB (solid) treatment groups showing the statistical significance at times $t = 15, 30, 45, 60, 90, 120$ and 150 min, **C** P_aO₂ (red), ($p = 0.0117, 0.0124, 0.0137, 0.0058, 0.0014, 0.0022$ and 0.0005), **D** P_{mv}O₂ (blue), ($p = 0.0138, 0.0597, 0.0799, 0.1568, 0.1230, 0.0171$ and 0.0110), **E** SpO₂ (violet), ($p = 0.1350, 0.1239, 0.0788, 0.0329, 0.0212, 0.0095$ and 0.0133), **F** P_aCO₂ (gold), ($p = 0.0025, 0.0004, <0.0001, <0.0001, 0.0109, <0.0001$ and 0.0003), **G** P_{mv}CO₂ (green), ($p = 0.0330, 0.0113, 0.0132, 0.0007, 0.0030, 0.0009$ and 0.0018) and **H** ETCO₂ (teal), ($p = 0.0040, 0.0269, 0.0136, 0.0007, 0.0004, 0.0015$ and 0.0012)

(OMB Δ P_aCO₂ = -10.0 ± 6.4 mmHg, NT Δ P_aCO₂ = 5.4 ± 4.6 mmHg) and remained lower out to 150 min at 53.6 ± 5.6 mmHg (OMB Δ P_aCO₂ = -19.7 ± 7.6 mmHg, NT Δ P_aCO₂ = 17.9 ± 11.7 mmHg). P_{mv}CO₂ (Fig. 3B, G) was statistically lower for animals receiving OMB therapy at 15 min (OMB Δ P_{mv}CO₂ = -0.2 ± 4.4 mmHg, NT Δ P_{mv}CO₂ = 6.2 ± 3.5 mmHg) and 150 min (OMB Δ P_{mv}CO₂ = -7.6 ± 6.7 mmHg, NT Δ P_{mv}CO₂ = 18.3 ± 11.2 mmHg). The ETCO₂ measurements showed a similar decline for the animals receiving OMB from 15 min (OMB Δ ETCO₂ = -5.3 ± 4.8 mmHg, NT Δ ETCO₂ = 4.2 ± 3.8 mmHg) out to 150 min (OMB Δ ETCO₂ = -9.6 ± 3.9 mmHg, NT Δ ETCO₂ = 15.0 ± 10.2 mmHg, Fig. 3B, H).

Effect of OMB treatment on lung parenchyma, inflammatory cytokines and proteomics

No significant changes were observed in lung injury score and wet/dry weight ratio at the 3 h time point (Fig. 4A–D). However, we observed a significant increase in IL-1 β levels in immunoblotting of lung tissue lysates at 48 h post-smoke inhalation in smoke injury (SI) animals compared to the control animals (Figs. 4E, F, 5). Expression

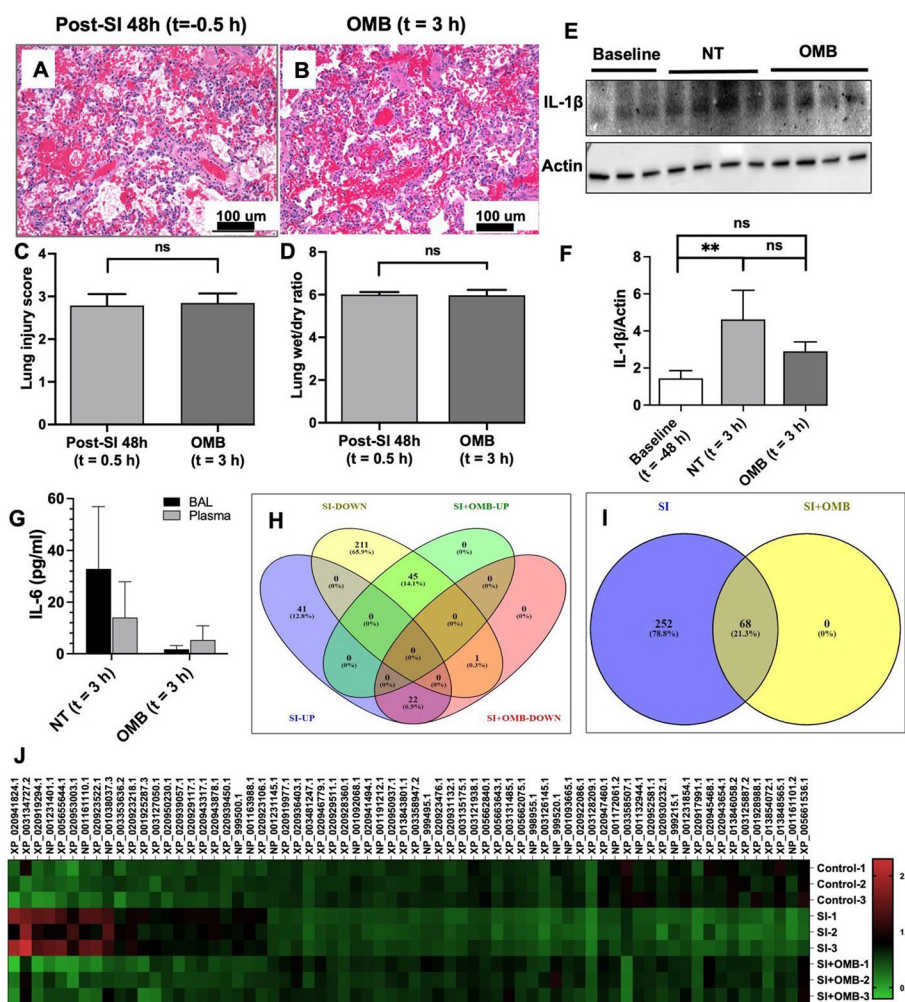


Fig. 4 Local and systemic injury and inflammation. Hematoxylin and eosin (H&E) staining of paraffin-embedded lung tissue sections of SI + 48 h ($t = -0.5$ h) (A) and OMB treatment ($t = 3$ h) (B) animals (scale bar = 100 μm). Comparison of lung injury score (C) and lung wet/dry ratios (D) between SI + 48 h ($t = -0.5$ h) and OMB treatment ($t = 3$ h) samples. E, F Immunoblot analysis of IL-1β expression levels in fresh frozen lung tissues of baseline ($t = -48$ h), NT and OMB samples ($t = 3$ h). Difference between baseline and NT groups was statistically significant ($p = 0.0092$). G IL-6 marker analysis for NT and OMB ($t = 3$ h) for BAL and plasma samples. H–J Proteomic analysis of control ($t = -48$ h), SI (NT, $t = 3$ h) and SI + OMB ($t = 3$ h) groups for their global protein expression as described in Materials and Methods section. Venn diagram showed 320 proteins with significant differential expression between SI and OMB groups (H, I). Heat map analysis of 68 proteins that were significantly upregulated or downregulated at 3 h post-OMB treatment (J). A p value of < 0.05 was considered statistically significant

status of both cytokines was reversed at 3 h post-OMB treatment (Fig. 4F), indicating an anti-inflammatory effect of OMB. There were lower IL-6 levels for the OMB group (BAL = 1.7 ± 1.5 pg/mL, plasma = 5.3 ± 5.5 pg/mL) as compared to the NT group (BAL = 32.9 ± 24.0 pg/mL, plasma = 14.0 ± 13.9 pg/mL) for both the BAL and plasma samples (Figs. 4G, 5).

Lung tissues of control, SI and SI with OMB groups were compared for their global protein expression by proteomic analysis. Several proteins were differentially expressed between these groups. Of these proteins, 320 proteins were significantly upregulated or downregulated at 48 h post-smoke exposure compared to control. Interestingly, at 3 h

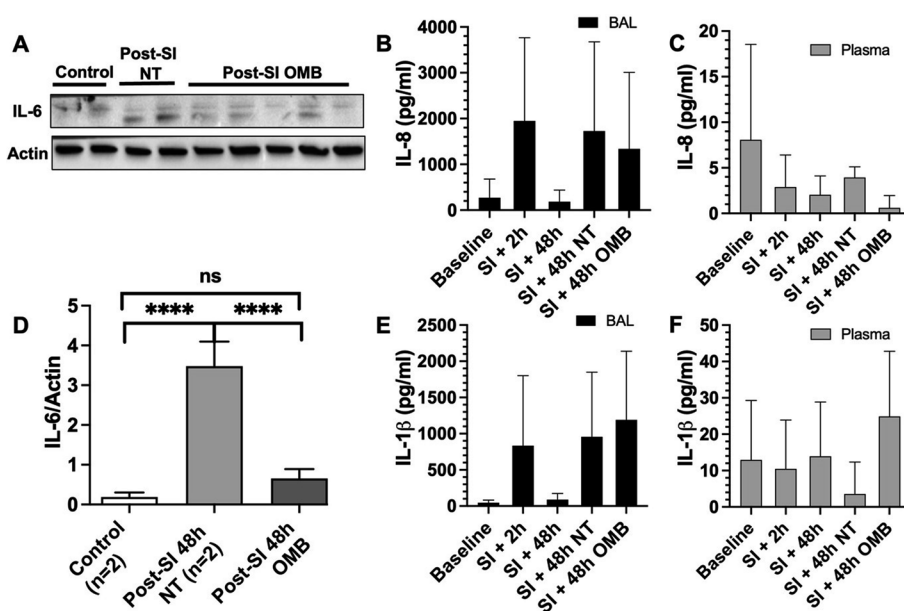


Fig. 5 IL-6 immunoblot and IL-8 and IL-1 β ELISA analysis. **A, D** Immunoblot analysis of IL-6 expression levels in lung tissues of Control ($t = -48$ h), SI ($t = -46$ h) and SI + OMB ($t = 3$ h) groups ($p < 0.0001$). **B, C** IL-8 expression level in BAL fluid and plasma samples of treated animals at baseline ($t = -48$ h), SI + 2 h ($t = -46$ h), SI + 48 h ($t = -0.5$ h), NT and OMB ($t = 3$ h) samples. **E, F** IL-1 β expression level in BAL fluid and plasma samples of treated animals at the same timepoints as IL-8 analysis

post-OMB treatment, the expression status of these 320 proteins was partially reversed, and we observed a significant differential expression of 68 proteins compared to SI animal tissue samples as shown by the Venn diagrams (Fig. 4H, I) and heat map analysis (Fig. 4J).

Discussion

The primary driving force behind systemic oxygenation with OMB treatment is diffusion. Upon delivery to the colon, the OMBs comprising 95–98% oxygen gas deliver oxygen to hypoxic tissue with a diffusivity of $\sim 2.4 \times 10^{-6} \text{ cm}^2/\text{s}$ [16]. OMBs are superior for delivering oxygen as compared to a macro, non-shelled oxygen gas bubble due to their ability to intimately spread and mix throughout the colon submucosa and increase the gas: liquid surface area. This enhancement in transport for microbubbles has led to their utilization in industrial fermentation [17–19], and other applications requiring rapid gas absorption. The colon walls are highly vascularized and absorptive (removing ~ 2 L/day of water from chyme and stool [20]) and thereby allow oxygen and carbon dioxide to diffuse across the submucosa from the lumen to adjacent tissue. Within the colon tissue, oxygen diffuses into capillary vessels, binds to deoxygenated blood, and circulates, resulting in augmentation of systemic oxygen levels. The statistically significant rises in oxygen blood gas sampled at the carotid and pulmonary arteries demonstrate that colonic OMBs can deliver systemic oxygen to a patient via the systemic and splanchnic circuits.

The diffusion mechanism responsible for delivering systemic oxygen to an OMB-treated patient is also responsible for removing systemic CO₂. The permeability of CO₂

in tissue is ~20-fold higher than for oxygen [21]. Thus, CO₂ counter-diffuses into the OMB microfoam as O₂ diffuses into tissue, and the OMB structure is stabilized during this gas-exchange process by the structural integrity of the lipid shell [22]. As hypercapnic venous blood passes through the systemic and splanchnic circuits, it sheds CO₂ into the OMB matrix. This lowering of CO₂ blood gas in the mixed venous return, verified by both P_{mv}CO₂ and ET_{CO2} (Fig. 3B, E, H), reduces the alveolar CO₂ that would otherwise dilute alveolar O₂, thereby increasing P_AO₂ (Fig. 6). Conversely, all NT animals experienced an increase in CO₂ levels throughout the study.

In this study, we showed that colonic OMB can improve systemic O₂ delivery and CO₂ removal for up to 150 min. This time duration is relevant for acute, severe hypoxia as a possible bridge to alternate therapy, where resources or access is limited, or when the risks of pulmonary bypass via established methods outweigh the benefit. Eventually the OMB bolus will deplete its oxygen supply and saturate itself with CO₂. In such cases, multiple bolus administrations can be administered, where the expired bolus can be flushed naturally or with the help of conventional pro-motility enema. This capability favors colonic administration as the preferred enteral route for OMB therapy. In prior work, we focused on the intraperitoneal (IP) route in small animal lung injury models [6–8]. It is plausible that the peritoneal cavity may serve as an additional route to the colon to increase oxygenation further beyond what can be obtained by the colon alone. However, the colon route remains favorable because, for the same OMB dose range, the increase in systemic O₂ and decrease in CO₂ was similar for both routes, and the colon route has additional advantages of not requiring surgery to establish a port, the colon

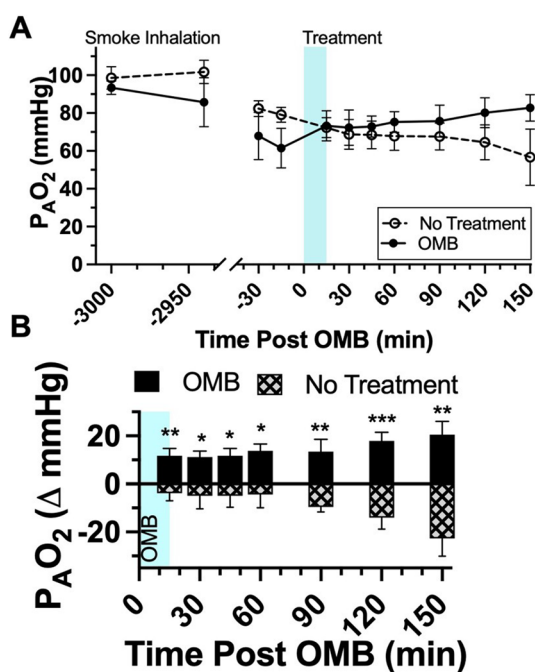


Fig. 6 Colonic OMB alveolar oxygen pressure. **A** P_AO₂ measurements for NT (dashed) and colonic OMB (solid) treatment groups from before smoke inhalation injury (t = -3000 min) out to t = 150 min post-treatment time. The change in P_AO₂ for NT (hashed) and OMB (solid) treatment groups showing the statistical significance at times t = 15, 30, 45, 60, 90, 120 and 150 min (p = 0.0046, 0.0328, 0.0186, 0.0201, 0.0078, 0.0009 and 0.0018)

can be easily flushed naturally or by enema and re-administered, and it requires only food-grade sterility since it is contained within the gastrointestinal tract. A potential complication of colonic administration of OMB therapy is injury or perforation of the colon or small intestine; neither complication was observed upon necropsy of our study animals.

We also found that OMB therapy for acute, profound hypoxemia resulted in the improvement of lung injury scores and systemic markers of inflammation; more detailed studies are needed to elucidate the mechanisms behind this potential treatment effect. Future studies by our investigational team will focus on the hypothesis that correction of systemic hypoxia with OMB therapy mitigates the deleterious effects of profound hypoxemia.

The main limit of this study is that we examined effects out to a pre-determined 150 min endpoint. Severe hypoxia from respiratory distress may occur for a much longer period, over days and even weeks. Therefore, future work will focus on understanding not only the therapeutic duration of a single OMB bolus, but also the therapeutic effects of multiple doses. Additionally, colonic OMB therapy should be tested in alternative large-animal ARDS models, such as lipopolysaccharide and oleic acid, with varying degrees of severity of lung insult and hypoxia, as well as the interaction between OMB therapy and mechanical ventilation. Colonic OMB therapy should also be investigated as a bridge to ECMO for rapidly deteriorating patients who require additional time for transport or to set up the circuit, or for austere environments with limited resources.

Conclusions

We show that colonic oxygen microbubble therapy provides significant systemic oxygenation and carbon dioxide removal for at least 150 min following administration. Future research is needed to detail potential mechanisms of treatment effect, impact on intestinal microbiota, as well as any associated risks of those effects for hypoxemic patients.

Acknowledgements

We would also like to acknowledge Andrew Kingsbury for generating the schematics presented in this manuscript.

Author contributions

Conceptualization: PAM, RMS, MAB, KLB. Methodology: PAM, PDL, RTS, DN, MAB, KLB. Investigation: PAM, PDL, HRW, AM, RTS, EMD, JC, DN, KLB. Visualization: PAM, PDL, HRW, MAB, KLB. Funding acquisition: MAB, KLB. Project administration: PAM, RMS, MAB, KLB. Supervision: PAM, MAB, KLB. Writing—original draft: PAM, PDL. Writing—review and editing: PAM, PDL, MAB, KLB. All authors read and approved the final manuscript.

Funding

This study was supported by the Department of Defense US Air Force award number FA4600-18-D-9001. DOD Joint Program Committee 6/Combat Casualty Care Research Program. The views expressed are those of the authors and do not reflect the official views or policy of the Department of Defense or its Components. This study was conducted under a protocol reviewed and approved by the USAF 59th Medical Wing IRB and in accordance with the approved protocol. This study was also supported by the National Institutes of Health award R01HL151151 awarded to Mark A. Borden.

Availability of data and materials

The datasets used and/or analyzed during the current study are available from the corresponding author on reasonable request.

Declarations

Ethics approval and consent to participate

All animal experiments were approved and supervised by the University of Nebraska-Lincoln Institutional Animal Care and Use Committee.

Consent for publication

Not applicable.

Competing interests

Authors PAM, RMS, RTS, MAB, and KLB have financial holdings in the company Respirogen, Inc. in the form of stock and stock option agreements. MAB is a Founder and Chief Scientific Officer of Respirogen, Inc. Respirogen, Inc. looks to commercialize the oxygen microbubble technology.

Received: 20 December 2022 Accepted: 2 May 2023

Published online: 26 June 2023

References

1. Máca J, Jor O, Holub M, Sklienka P, Burša F, Burda M, Janout V, Ševčík P (2017) Past and present ARDS mortality rates: a systematic review. *Respir Care* 62:113–122
2. Matthay MA, Zemans RL, Zimmerman GA, Arabi YM, Beitler JR, Mercat A, Herridge M, Randolph AG, Calfee CS (2019) Acute respiratory distress syndrome. *Nat Rev Dis Prim* 5:1–22
3. CDC (2020) COVID data tracker. Centers for Disease Control and Prevention. <https://covid.cdc.gov/covid-data-tracker>
4. Guo L, Jin Z, Gan TJ, Wang E (2021) Silent hypoxemia in patients with COVID-19 pneumonia: a review. *Med Sci Monit* 27:e930776
5. Gattinoni L, Marini JJ, Collino F, Maiolo G, Rapetti F, Tonetti T, Vasques F, Quintel M (2017) The future of mechanical ventilation: lessons from the present and the past. *Crit Care* 21:183
6. Feshitan JA, Legband ND, Borden MA, Terry BS (2014) Systemic oxygen delivery by peritoneal perfusion of oxygen microbubbles. *Biomaterials* 35:2600–2606
7. Legband ND, Feshitan JA, Borden MA, Terry BS (2015) Evaluation of peritoneal microbubble oxygenation therapy in a rabbit model of hypoxemia. *IEEE Trans Biomed Eng* 62:1376–1382
8. Fiala C, Slagle N, Legband F, Aghabaglou K, Buesing M, Borden S, Harris B (2020) Terry, treatment of a rat model of LPS-induced ARDS via peritoneal perfusion of oxygen microbubbles. *J Surg Res* 246:450–456
9. Albenberg L, Esipova TV, Judge CP, Bittinger K, Chen J, Laughlin A, Grunberg S, Baldassano RN, Lewis JD, Li H, Thom SR, Bushman FD, Vinogradov SA, Wu GD (2014) Correlation between intraluminal oxygen gradient and radial partitioning of intestinal microbiota. *Gastroenterology* 147:1055–1063.e8
10. <https://www.biorxiv.org/content/10.1101/2021.12.08.466665v1#:~:text=Colonic%20OMB%20infusion%20%2875%20%E2%80%93%20100%20mL%20Fkg%20dose%29,of%2012.9%25%20%C2%B1%2018.7%25%20over%20the%20same%20timeframe>
11. Leiphrakpam PD, Weber HR, McCain A, Matas RR, Duarte EM, Buesing KL (2021) A novel large animal model of smoke inhalation-induced acute respiratory distress syndrome. *Respir Res* 22(1):198. <https://doi.org/10.1186/s12931-021-01788-8>
12. Amato MB, Meade MO, Slutsky AS, Brochard L, Costa EL, Schoenfeld DA, Stewart TE, Briel M, Talmor D, Mercat A, Richard JC, Carvalho CR, Brower RG (2015) Driving pressure and survival in the acute respiratory distress syndrome. *N Engl J Med* 372(8):747–755
13. Chiumello D, Carlesso E, Brioni M, Cressoni M (2016) Airway driving pressure and lung stress in ARDS patients. *Crit Care* 20(1):276
14. Neto AS, Hemmes SN, Barbas CS, Beiderlinden M, Fernandez-Bustamante A, Futier E, Gajic O, El-Tahan MR, Al Ghamdi AA, Günay E, Kokulu S, Kozian A, Jaber S, Licker M (2016) Association between driving pressure and development of postoperative pulmonary complications in patients undergoing mechanical ventilation for general anaesthesia: a meta-analysis of individual patient data. *Lancet Respir Med* 4(4):272–280
15. Gattinoni L, Tonetti T, Cressoni M, Cadringer P, Herrmann P, Moerer O, Protti A, Gotti M, Chiurazzi C, Carlesso E, Chiumello D, Quintel M (2016) Ventilator-related causes of lung injury: the mechanical power. *Intensive Care Med* 42(10):1567–1575
16. Valentin JE, Freytes DO, Grasman JM, Pesyna C, Freund J, Gilbert TW, Badylak SF (2009) Oxygen diffusivity of biologic and synthetic scaffold materials for tissue engineering. *J Biomed Mater Res A* 91A:1010–1017
17. Bredwell MD, Worden RM (1998) Mass-transfer properties of microbubbles. 1. Experimental studies. *Biotechnol Prog* 14:31–38
18. Bangalore DV, Bellmer DD (2006) Microbubbles for enhancement of oxygen transfer in xanthan gum fermentation. *Chem Eng Commun* 193:1232–1252
19. Dai Y, Deng T, Wang J, Xu K (2004) Enhancement of oxygen gas–liquid mass transfer with colloidal gas aiphron dispersions. *Colloids Surf A* 240:165–171
20. Saltzman WM (2015) *Biomedical engineering: bridging medicine and technology*. Cambridge University Press, Cambridge
21. Wright CI (1934) The diffusion of carbon dioxide in tissues. *J Gen Physiol* 17:657–676
22. Kwan JJ, Borden MA (2012) Lipid monolayer dilatational mechanics during microbubble gas exchange. *Soft Matter* 8:4756–4766

Publisher's Note

Springer Nature remains neutral with regard to jurisdictional claims in published maps and institutional affiliations.